

# Design of a next generation synoptic solar observing network: solar physics research integrated network group (SPRING)

Sanjay Gosain<sup>a</sup>, Markus Roth<sup>b</sup>, Frank Hill<sup>a</sup>, Alexei Pevtsov<sup>a</sup>, Valentin M. Pillet<sup>a</sup>, and Michael J. Thompson<sup>c</sup>

<sup>a</sup>National Solar Observatory, 3665 Discovery Drive, Boulder, CO 80303, USA

<sup>b</sup>Kiepenheuer-Institut für Sonnenphysik, Schneckstr. 6, 79104 Freiburg, Germany

<sup>c</sup>National Center for Atmospheric Research, 1850 Table Mesa Dr, Boulder, CO 80305, USA

## ABSTRACT

Long-term synoptic observations of the Sun in different wavelength regions are essential to understand its secular behavior. Such observations have proven very important for discovery of 11 year solar activity cycle, 22 year magnetic cycle, polar field reversals, Hale’s polarity law, Joy’s law, that helped Babcock and Leighton to propose famous solar dynamo model. In more recent decades, the societal impact of the secular changes in Sun’s output has been felt in terms of solar inputs to terrestrial climate-change and space-weather hazards. Further, it has been realized that to better understand the activity phenomena such as flares and coronal mass ejections (CMEs) one needs synoptic observations in multiple spectral lines to enable tomographic inference of physical parameters.

Currently, there are both space and ground based synoptic observatories. However, given the requirements for the long-term stability and reliability of such synoptic datasets, ground-based facilities are more preferable. Also, the ground based observatories are easy to maintain or upgrade while detailed and frequent calibrations are easily possible. The only ground-based facility that currently provides full-disk velocity and magnetic field maps of the Sun around the clock and at good cadence, is the Global Oscillations Network Group (GONG) network of National Solar Observatory (NSO) which is operational since the mid 90s.

Due to its aging instrumentation, operating for nearly three decades, and new requirements to obtain multi-wavelength observations, a need is felt in the solar community to build a next generation synoptic observatory network. A group of international observatories have come together under the auspices of SOLARNET program, funded by European Union (EU), to carryout a preliminary design study of such a synoptic solar observing facility called “SPRING”, which stands for Solar Physics Research Integrated Network Group. In this article we will present concept of SPRING and the optical design concept of its major instruments.

**Keywords:** Sun; Synoptic; Optical Design; Network; Space-Weather; Polarimetry

## 1. INTRODUCTION

### 1.1 Science Goals:

The science Goals for the SPRING network are as follows:

- Solar Dynamo: Long-term accurate monitoring of solar magnetic and velocity fields for characterization of solar cycle from activity latitudes to poles for constraining solar dynamo models.
- Space Weather: Evolution of magnetic and velocity fields in active regions (AR), that lead to eruptive phenomena. Relation of flux emergence, cancellation, non-potentiality to flare occurrence.
- Atmospheric Seismology: Subsurface flows, wave propagation in solar chromosphere, chromospheric heating.

---

Further author information: (Send correspondence to A.A.A.)

A.A.A.: E-mail: aaa@tbk2.edu, Telephone: 1 505 123 1234

B.B.A.: E-mail: bba@cmp.com, Telephone: +33 (0)1 98 76 54 32

- Inconstant Sun: Sun-as-a-star spectra, solar irradiance, solar diameter.
- Context Imager: High resolution broadband and narrowband images for context information for coordinated data analysis with other observatories such as large aperture solar telescopes and space observatories.

## 1.2 Observational Requirements:

The science goals translate into following observational requirements:

- Field of view: To cover full-disk and prominences at limb (0.65 degrees)
- Spatial Resolution: 1 arc-sec angular resolution for seeing-limited observations with fast tip-tilt guiding.
- Spectral Resolution: Typical solar photospheric lines require spectral resolution of  $\sim 50,000 - 150,000$  from 500 to 1540 nm, respectively. This corresponds to FWHM: 0.01 nm.
- Temporal Resolution: 30 seconds for Dopplergrams and 10 minutes for Magnetograms.
- Spectral Lines: Fe I 525, Fe I 617.3, Fe I 630 nm, Ca II 854.2 nm, He I 1083 nm, Fe I 1.5 micron (minimal).

## 2. DESIGN PHILOSOPHY

### 2.1 Continuous Observations:

Continuous observations from ground has many attractive features. Cost, maintenance, and easy upgrade are key factors. Such instrument networks can provide observations well over a solar cycle or longer. Having multiple identical instruments distributed globally are least affected, in general, from bad weather and equipment failures. The key question is to find optimal number of nodes in the network. Using modeling of climatological data, Hill and Newkirk (1985) showed that a six-site network could provide a duty cycle of 90% or more. GONG project has successfully demonstrated this concept for helioseismology studies.

### 2.2 Focus on space weather:

A network approach, similar to GONG, can also address the needs of space-weather research community. Space-weather forecasting for near-realtime solar wind conditions utilize numerical models that heavily depend upon magnetic field maps of the Sun, i.e., magnetograms, for their model inputs. Synoptic uninterrupted observations of the Sun enables real-time monitoring of the solar active regions, specially the vector magnetic fields in them, which are very important for driving space weather events such as solar flares and coronal mass ejections (CMEs). The current technology allows such real-time inference of solar magnetic fields, thanks to the availability of high-speed sensitive detectors and fast computational resources. SPRING will allow comprehensive measurement of solar magnetic fields, in different wavelengths, thereby sampling magnetic field at different heights in the solar atmosphere and build a tomographic 3D magnetic field inference in solar active regions. The SPRING should address this issue by providing vector magnetograms in near real-time, in multiple wavelengths.

From the same measurements that provide magnetic field parameters, we would also be able to get accurate velocity field maps, i.e., Dopplergrams, in multiple wavelengths. This will help in continuing helioseismology studies beyond GONG and will provide extra information about wave propagation in the solar chromosphere, interaction of waves with magnetic structures and their role in chromospheric heating.

### 2.3 Modular Approach:

It was clear from the start that SPRING would address a wide solar community and hence one single country or institute can not afford to build this network. Thus, a modular approach to build the instrument network must be adopted. A large equatorial tracking mount which can hold many different instruments in parallel is conceived. An example of such platform is the SOLIS instrument (Keller et al. 2003). The advantage of such approach is that the network can be developed at minimal cost by the community and individual countries or organizations can develop instruments of their interest and utilize the network instrument platform.

## 2.4 Data Rate and On-site Reduction

To derive magnetic and velocity fields on the Sun one typically needs to perform a spectral scan of solar absorption line and map intensity and polarization of the Zeeman components across it. To be able to acquire such observations one typically needs high spectral resolution (to resolve solar spectral lines, typically in sub-Angstrom range), a polarimeter (to measure Stokes vector,  $S = [I, Q, U, V]^T$ , across the spectral lines), and 2D detector (for spatial sampling of the full-disk of the Sun, half degree field-of-view). The data-cube thus obtained is a 4-dimensional data-cube, which is obtained as a function of time. Simple estimate of the data rate is as follows: Let  $N_s$  be the number of spectral lines and  $N_l$  number of wavelength samples across the line. Then for an angular resolution of 1 arc-sec, time cadence of 30 seconds, four Stokes parameters, one estimates the data rate as  $DR = N_s \times N_l \times 4 \times 2 \times 6 \times 32$  MB per minute. Assuming a six-site network, 32 MB per image, two data-cubes per spectral line per minute. For a modest selection of 8 spectral lines with 10 samples across the line, one estimates data rate of 1.3 GB per minute from the entire network, and this only includes dopplergrams and magnetograms. Broadband images and sun-as-a-star spectra are estimated to add another 0.7 GB per minute. So, in total one estimates about one TB per day per site or 6 TB data per day from the entire network. Of course, this can increase by a factor of two if more spectral lines are included.

The approach to manage such large amount of data would be to perform on-site data reduction and analysis/inversions of observed spectral profiles so as to transmit the final product, dopplergrams, magnetograms and intensitygrams to the central data station in near real-time. Further, with dedicated high-speed internet connection and using data compression techniques it will also be possible to download raw data at night from each site.

## 3. INSTRUMENT DESIGN

Before proceeding with the instrument design we need to know what are the observing parameters such as spatial, temporal and spectral resolutions, as well as range of these parameters. While resolution requirements are mentioned above the spectral range is governed by choice of spectral lines.

### 3.1 Choice of Spectral Lines

The initial selection of spectral lines is made on the basis of following arguments. The formation height of the spectral lines should sample a large range in the solar atmosphere, from deep photosphere to upper chromosphere. Further, the lines should have good sensitivity for Doppler measurements (Q-factor as defined in Bouchy et al., 2001) as well as good Zeeman sensitivity (product of Landé factor and wavelength,  $g_{eff}\lambda$ ). As a starting point, we select some candidate lines that have been used in the past for multi-height oscillation studies (Staiger 2011, Wiśniewska et al 2016). A tentative list of spectral lines considered at this stage for SPRING is given in Table 1.

### 3.2 Choice of Spectrometer

The choice of spectrometer to obtain the required observables is driven by sensitivity requirement for the measurements, time cadence (via throughput) and spatial resolution. Further requirements are (i) long term stability and durability, (ii) no impact on image quality and geometry, and (iii) rapid tunability.

Fundamentally there are two types of spectrometers which differ in the way the 4-D data-cube is gathered by them. These are, (i) filtergraphs, where 2D image is obtained instantaneously and scanning is done in wavelength domain such as Fabry-Perot interferometer (FPI), and (ii) slit spectrograph (SS), where 1D image and full spectra are obtained instantaneously and slit scanning is done in orthogonal spatial direction.

Time-cadence requirements ( $\sim 30$  seconds) rule out SS based concepts for high-cadence measurements, in general. However, spectrographs that use integrated field unit (IFU), such as fiber bundle, image slicer etc. or multi-slit spectrographs can overcome the cadence limitations to some extent. Even if cadence requirements can be met, the requirement for high geometric accuracy by helioseismology have not been demonstrated by the multislit-spectrographs.

It was thus realized that for high-cadence Doppler and magnetic field measurements FPI based system would be the instrument of choice. While for accurate spectral profiles and high SNR magnetic field maps in quiet sun

Table 1. List of spectral lines for observations with FDIS

Spectral line Å	Element	Formation Height (km)	Landé factor
3933	Ca II K		1.167
3968	Ca II H		1.333
5173	Mg I b1	595 ± 5	
5250	Fe I		3
5434	Fe I	556 ± 25	
5576	Fe I	310 ± 15	1.13
5890	Na I D2	927 ± 35	1.17
5896	Na I D1		1.33
6173	Fe I	276 ± 26	2.5
6301	Fe I	337 ± 23	1.67
6302	Fe I		2.49
6563	H I	1200-1700	1
6768	Ni I		1.43
7090	Fe I	284 ± 32	
8542	Ca II		1.1
10830	He I		
15648	Fe I		3

regions, albeit with much slower cadence, a slit based solution would be desirable. This slit based measurements in selected few spectral lines is also desirable from the point of view of consistency of the measurements with past synoptic records such as Kitt Peak Vacuum Tower (KPVT) and Synoptic Optical Long-term Investigations of the Sun/ VectorSpectroMagnetograph (SOLIS/VSM) magnetic field measurements, which are slit spectropolarimeter based.

A multi-slit full-disk spectroheliograph proof-of-concept was demonstrated by Lin (2016). In this article we do not describe this multi-slit concept to avoid duplication, and refer the reader to Lin (2016). In this article we will focus on the FPI based high-cadence Dopplergrams and magnetograms by SPRING. Both multi-slit and filter based instruments are planned for SPRING and would observe from a common tracking platform.

### 3.3 Fulldisk Imaging Spectropolarimeter: FDIS-B,R,IR

To meet the challenge of performing multi-line spectroscopy at a high cadence we follow the idea that the list of spectral lines should be divided into three broad spectral regions blue-red (300-600nm), red-nearIR (600-900) and nearIR-IR (900-1600nm). SPRING would then have three channels, each optimized for either blue, visible or infrared spectral region. Each channel optimizes its telescope design, pre-filters, FPI coatings, anti-reflection coatings, cameras spectral response, polarization optics etc. We call these systems: Fulldisk Imaging Spectropolarimeter (FDIS) with three channels, namely

- FDIS-B (blue): 3933, 3968, 5173, 5250, 5434 Å,
- FDIS-R (red): 5890, 5896, 6173, 6302, 6563, 6768 Å, and
- FDIS-IR (infrared): 8542, 10830, 15648 Å.

A conceptual layout of FDIS is shown in Figure 1. Top panel shows the front-end telescope RC-design telescope (RCT) equipped with active tip-tilt secondary (ATTS) mirror, feeding the instruments. The field-corrector lenses (FCL) are placed before the focal plane to provide aberration corrections over the FOV and wavelength range. The focal plane is telecentric which helps minimize field dependence in the optical components located near the primary focal plane, such as polarization calibration unit (PCU), prefilters (FW) and modulators (PM). Two FPIs (FP1 and FP2), in tandem, are placed in a collimated arrangement between collimating lens (CL) and imaging lens (IL). A beam splitter (BS) near PCU taps a small fraction of light (5%) for simultaneous white-light imaging camera (WLC) for contextual information, guiding signals to ATTS and for post-facto image

reconstruction of narrow-band FPI images. A polarizing beam splitter (PBS) near the science cameras CAM1 and CAM2 provide dual beam analysis of the modulated polarized light for minimizing seeing induced noise and utilizing photons in both beams for improved SNR. The collection of multi-line data via separate parallel channels has several advantages:

- Each telescope, filters, coatings, camera sensors can be optimized in a narrower spectral region than complete range, thereby reducing cost and improving performance.
- Same is true of the telescopes. Three smaller telescopes are cheaper than one large telescope.
- Redundancy of data collection. Even if one channel has technical failure other channels can still provide useful data for limited scientific objectives.
- Funding for each channel can be acquired by separate groups or by the same group in phased manner.
- For seeing limited full-disk observations larger aperture telescopes pose problem of blurring component, while smaller apertures (comparable to few times seeing value) see more of lower order errors in the wavefront that are easier to correct with online active optics or offline reconstruction methods.
- With large aperture telescopes observing large FOV the FPI apertures are also needed to be huge which drive the complexity and cost of the system.
- Simplicity of the light distribution system and more easy to maintain by remote sites. Easy to take the system on or off the equatorial mount for maintenance.

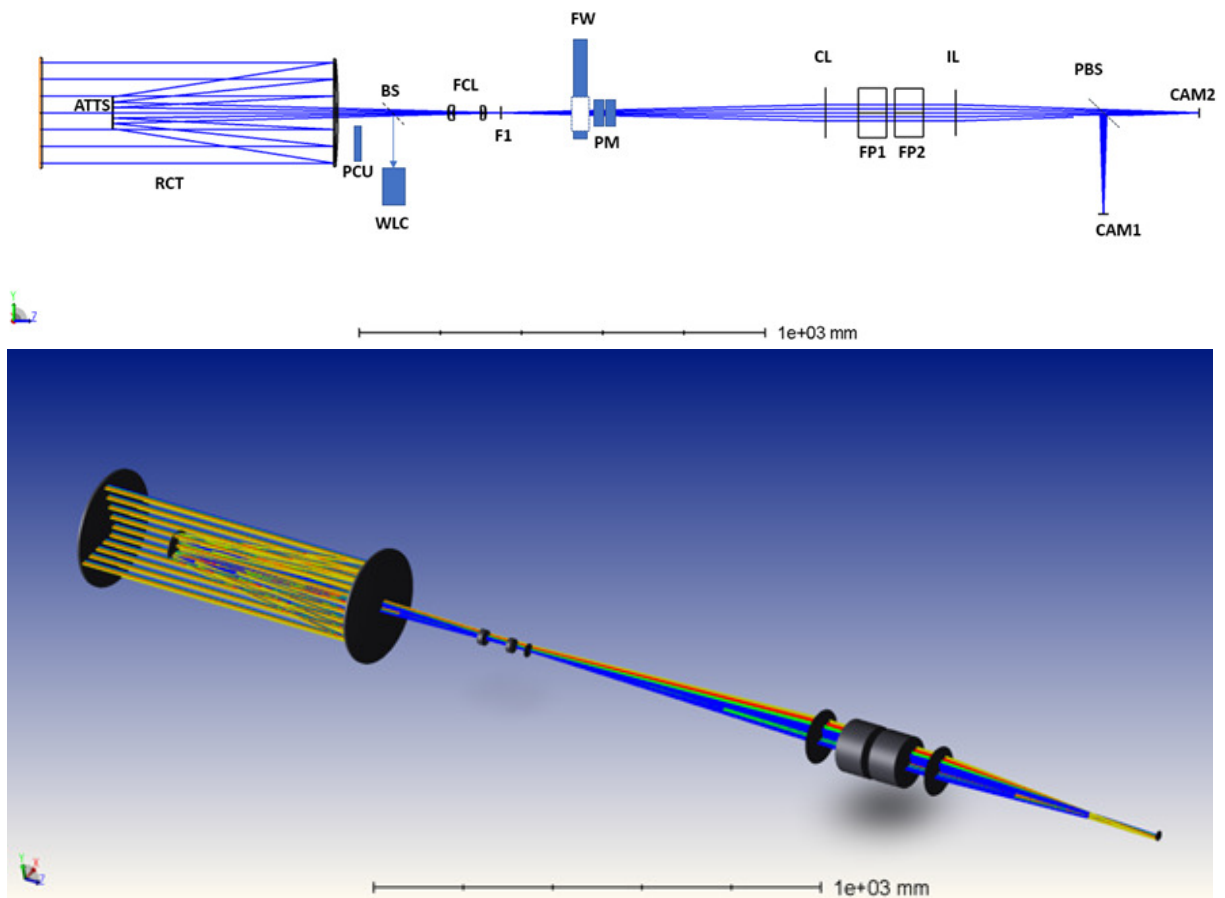


Figure 1. *Top panel* Schematic of FDIS system is shown. See text for details and labels. *Bottom panel:* A 3D visualization of the FDIS optical system using Zemax design tool.

### 3.4 Optical Design of the front-end

Variety of light feed systems were considered and finally a folded two mirror Ritchey-Chretien (RC) system, based on proven design of SOLIS/VSM front-end, was chosen. The rationale behind this choice was better optical performance over Schmidt-Cassegrain and Gregorian designs and compact size compared to an achromatic lens.

An aperture size of 26 cm was chosen for considerations of SNR and cadence requirements. The effective focal length of 3.33 m gives a  $f/13$  system. The design was done using Zemax software and was optimized for wavelength from 0.5 to 1.5 micron. The design parameters of FDIS are given in Table 2. The optical layout of the system is given in Figure 2. A field corrector lens is used to minimize aberrations over the FOV. The corresponding spot diagram is shown in Figure 3 for all field angles and design wavelengths. The secondary mirror diameter is about 30% of the primary. Back focal distance from the secondary is 35 cm, which provides ample space for accommodating calibration filters. The secondary mirror would be mounted on a tip-tilt platform for real-time correction of alignment, tracking and global wavefront tip-tilt errors.

The primary mirror would be made of ultra-low expansion (ULE) material to minimize temperature induced aberrations. The mirror coating would be overcoated silver for high reflectance in visible and near-infrared (NIR). The secondary mirror would be a single Silicon crystal (as in SOLIS/VSM). Regular glass based mirrors with their low thermal conductivity lead to large thermal gradients within mirror substrate that would lead to significant optical aberrations due to high radiative flux. Near the prime focus a two lens field corrector provides adequate image quality over the whole field-of-view (FOV), minimal geometric distortions, homogenous image size for all wavelengths, and a quasi-telecentric beam to minimize field effects in subsequent near-focal plane optics, i.e., the modulator and order sorting prefilter. Symmetric optical design of the telescope helps in minimizing the instrumental polarization.

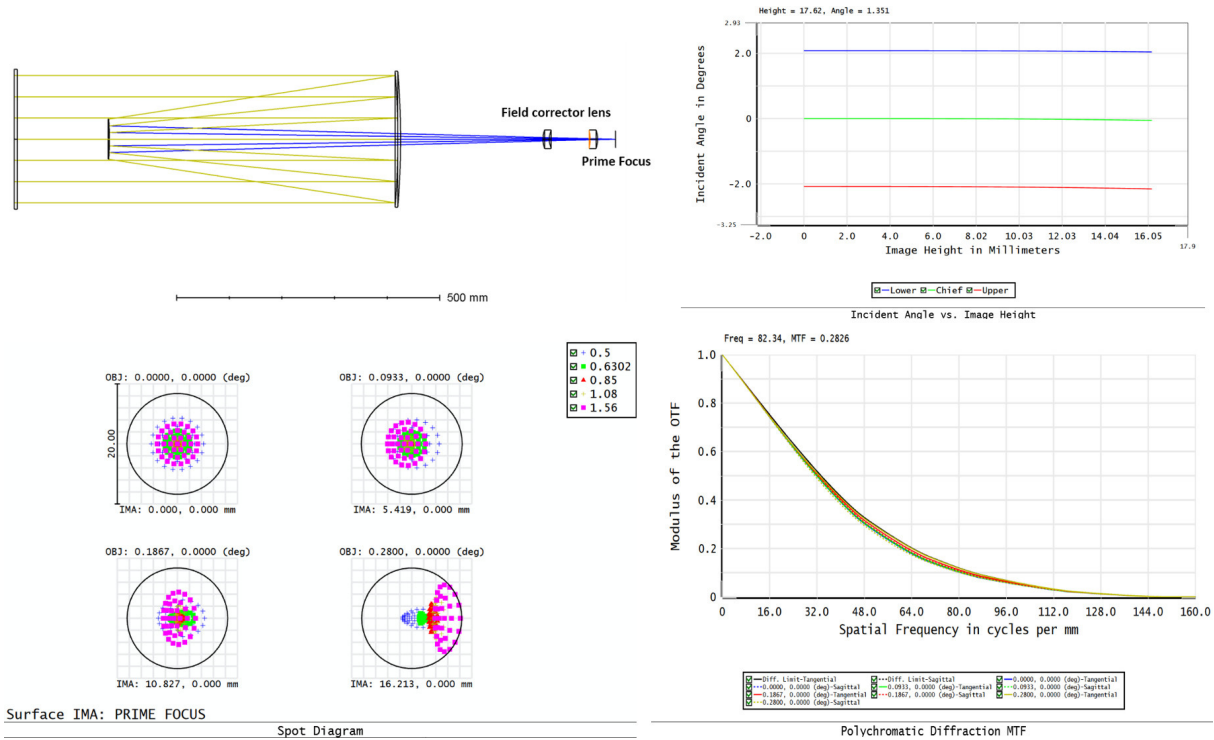


Figure 2. *Top left:* Zemax model of the FDIS telescope folded optics design. *Bottom left:* Spot diagram for various field angles and design wavelengths. *Top right:* Telecentricity of the image plane is shown with chief ray angle versus image height plot. *Bottom right:* Modulation Transfer Function (MTF) of the telescope at various wavelengths along with diffraction limited MTF in black color.

Table 2. Parameters of the FDIS Telescope

Parameter	Value
Entrance Aperture Diameter	254 mm
Secondary Diameter	80 mm (32% of Primary)
Maximum Field of View	0.28 degrees
Effective focal length	3327 mm
Image space F#	13
Back Focal Distance	34 mm
Solar Disk Diameter	32 mm
Wavelengths optimized	0.5, 0.63, 0.85, 1.08, 1.56 microns
Image Plane	Telecentric

### 3.5 Design of Tandem FPI Imaging Spectrograph

The choice of using FPI over other tunable filter options was made with following considerations. FPI offers (i) high throughput, (ii) rapid wavelength tunability with high degree of repeatability (with real-time laser fed calibrations), (iii) well understood data calibration, (iv) proven technology in solar astronomy, (v) robustness, and (vi) compactness. There are various examples of such FPIs used in solar astronomy, such as, in IBIS (Cavallini 2006), TESOS (Kentischer et al. 1998), GFPI (Puschmann et al. 2012), IMAX (Martinez-Pillet et al. 2011), CRISP/SST (Scharmer 2006), Hellride (Staiger 2008) and USO/VSM (Gosain et al. 2006). These FPI's can be either solid or air gap etalons. For robustness, free-spectral range, rapid tunability and lifetime concerns, air-gap, piezo-driven, servo-parallelized, which are commercially available are chosen.

An important choice that must be made regarding FPIs is the mounting configuration for FPIs. There are two options available, i.e., telecentric or collimated mounting. Here a trade-off must be made between, nonuniformity of FPI transmission profile over FOV (telecentric) versus uniformity of transmission profile over FOV but spectral shift across the FOV (collimated). Clearly, the former requires frequent detailed characterization of FPI transmission profile variations over FOV and presents more complicated data reduction procedure, while the latter is much simpler and passband shift across FOV is easy to tackle in data acquisition and reduction. Further, collimated system can be more compact than the telecentric mounting design for a given spectral resolution and FOV. The FPI in three FDIS channels would be optimized for high performance by designing dielectric coatings on the etalon plates optimally for the given wavelength range.

Further, for tandem FPI configuration a study of optimum spacing ratio of the two etalons is carried out for the three FDIS channels. The optimum ratio is obtained such that the net stray light from adjacent overlapping transmission channels of the two FPI is minimized while the signal in the common transmission channel of two FPI is maximized, as described in Cavallini et al. (2006). Table 3 gives the computed optimum spacing ratios for the tandem FPIs in the three FDIS channels.

The choice of aperture of the FPI is made from the trade-off between cadence requirement, SNR, mass of FPI plates and related flexure issues on a tracking mount, passband shift across the FOV. Figure 3 (bottom panel) shows maximum passband-shift across FOV for various spectral lines with different FPI apertures, for a given telescope aperture (25 cm). In general the passband shift increases with wavelength. This necessitates performing extra wavelength sampling blue-wards of the spectral line.

Based on the study of impact of this extra scanning required for various FPI apertures while simultaneously maintaining the SNR and cadence requirements we arrived at an optimal diameter of the FPI aperture as 10 cm. With the 25 cm aperture telescope and 10 cm aperture FPI we can reach requirement of observing each spectral line with velocity sensitivity of 20 m/s or better for photospheric lines and less than 50 m/s for broader chromospheric lines (as shown in top panel of Figure 3). Further for He I 1083nm line a sensitivity of about 200m/s is reached due to its shallow and broad shape. Since velocity amplitude in chromospheric layers is easily several times larger than photospheric oscillations, basically due to its lower density, this is not an issue.

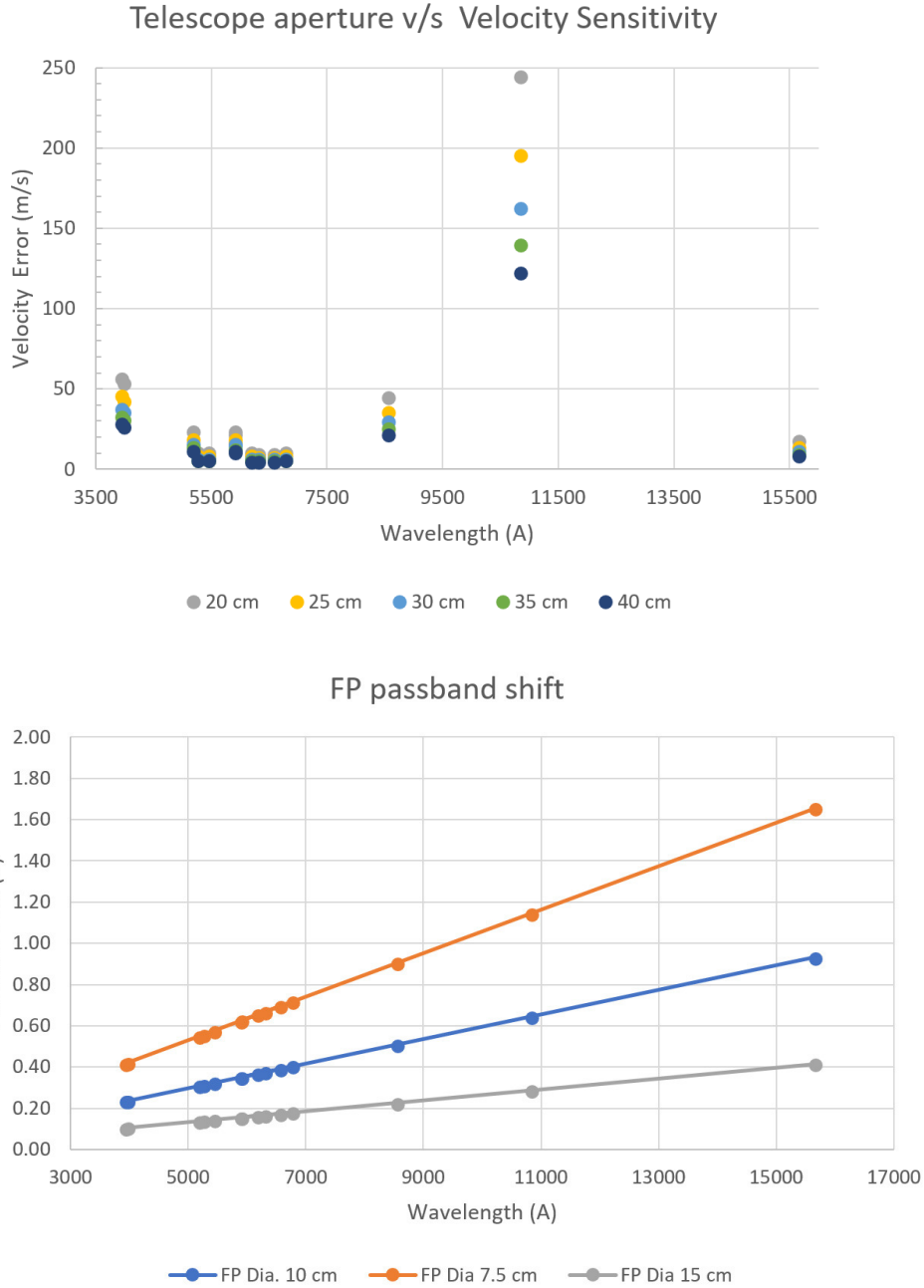


Figure 3. *Top panel:* The choice of telescope aperture and its effect on the velocity sensitivity for various spectral lines is shown. *Bottom panel:* The choice of FPI aperture and its effect on maximum passband shift at the edge of the FOV is shown for various spectral lines.

### 3.6 Expected Performance

The three FDIS channels mentioned above can be mounted adjacent to each other on a common platform atop equatorial mount. Further, these FDIS instruments can observe in parallel and meet the requirement of obtaining multi-line dataset at a cadence of 30 seconds. The SNR studies show that the sensitivity for dopplergrams and longitudinal magnetograms is adequate, however, it is not enough for transverse component of the magnetic field. This is because the transverse Zeeman effect induced linear polarization signal is proportional to square



Table 3. FPI cavity ratios for the three channels FDIS-B, R and IR.

Channel	Cavity Length (microns)
FDIS-B	
FP1	216
FP2	540
FDIS-R	
FP1	416
FP2	1040
FDIS-IR	
FP1	1400
FP2	3500

of the transverse field. Since the vector magnetograms do not require 30 second cadence, rather a cadence of 10 minute or so, which seems adequate for space weather research, an offline accumulation of Doppler shift corrected spectropolarimetric scans would be able to provide 5 times more SNR, which would be adequate for vector magnetograms of active regions. On the other hand, as mentioned earlier, high sensitivity measurements of vector magnetic fields in quiet regions, such as outside active regions and polar regions would require multi-slit spectrograph based instrument such as described in Lin (2014) and would be compatible with past measurements from NSO/KPVT and SOLIS/VSM which date back to 1970s. Such multi-pronged strategy for instrumentation development would allow SPRING to address different spatial and temporal scales of solar magnetism and dynamics.

### 3.7 Acknowledgments

The SPRING design presented in this article was carried out by author SG, with inputs from various coauthors and other numerous SOLARNET partners, funded by European Union's (EU) Seventh Framework Program (FP7). Local hospitality and scientific discussions by colleagues at Kiepenheuer Institut for Sonnenphysik (KIS) at Freiburg, Germany, and their permission to utilize telescope time at Vacuum Tower Telescope (VTT), Tenerife, Spain, for some of the feasibility studies for SPRING is acknowledged. Leave from National Solar Observatory (NSO) to visit KIS for carrying out this work is also acknowledged. Finally, we acknowledge (late) Joe Staiger, who participated in various SPRING feasibility studies at VTT.

### 3.8 References

#### REFERENCES

- [1] Gosain, S., Venkatakrishnan, P., & Venugopalan, K. 2006, *Journal of Astrophysics and Astronomy*, 27, 285
- [2] Hill, F., & Newkirk, G., Jr. 1985, *Solar Physics*, 95, 201
- [3] Keller, C. U., & SOLIS Team 2003, *Bulletin of the American Astronomical Society*, 35, 20.23
- [4] Bouchy, F., Pepe, F., & Queloz, D. 2001, *A&A*, 374, 733
- [5] Wiśniewska, A., Musielak, Z. E., Staiger, J., & Roth, M. 2016, *ApJL*, 819, L23
- [6] Staiger, J. 2011, *A&A*, 535, A83
- [7] Lin, H. 2014, *Proc. of SPIE*, 9147, 914712
- [8] Cavallini, F. 2006, *Solar Physics*, 236, 415
- [9] Puschmann, K. G., Denker, C., Kneer, F., et al. 2012, *Astronomische Nachrichten*, 333, 880
- [10] Staiger, J. 2011, *A&A*, 535, A83
- [11] Kentischer, T. J., Schmidt, W., Sigwarth, M., & Uexkuell, M. V. 1998, *A&A*, 340, 569
- [12] Scharmer, G. B., Narayan, G., Hillberg, T., et al. 2008, *ApJL*, 689, L69
- [13] Martínez Pillet, V., Del Toro Iniesta, J. C., Álvarez-Herrero, A., et al. 2011, *Solar Physics*, 268, 57